On evolution of Primary Cosmic Ray mass composition in the energy region $10^{14} - 10^{16}$ eV

Yu.F. Novoseltsev[1*] and G.M. Vereshkov[1,2†]
[1] *Institute for Nuclear Research of Russian Academy of Sciences, 60th October Anniversary Prospect, 7a, 117312 Moscow, Russia and*
[2] *Research Institute of Physics, Southern Federal University, Stachki Prospect, 194, 344090 Rostov-on-Don, Russia*

A new method of determining Primary Cosmic Ray mass composition is proposed. The method is based on quasi-localization of the integral equation for the Extensive Air Showers spectrum versus the total number of high energy muons ($E_\mu \geqslant 235$ GeV) and an expansion of the experimentally measured spectrum in spectra of five group of primary nuclei. The cosmic ray mass composition is established in the energy region $10^{14} - 10^{16}$ eV. In the region $10^{15} - 10^{16}$ eV our analysis points to a lightening of the mass composition from $p + \alpha \simeq 0.54$, $\langle \ln A \rangle \simeq 1.97$ to $p + \alpha \simeq 0.69$, $\langle \ln A \rangle \simeq 1.56$.

PACS numbers: 26.40.+r

I. INTRODUCTION

We present a new method of analysis of data on the Extensive Air Showers (EAS) spectrum versus the total number of high energy muons, $I(n \geqslant n_\mu)$, to determine the primary cosmic ray (CR) mass composition. We use the data on high multiplicity muon events ($n_\mu \geqslant 114$, $E_\mu \geqslant 235$ GeV) collected at the Baksan underground scintillation telescope [1, 2]. In [2] the muon multiplicity spectrum (i.e. the number m of muons hitting the facility at an unknown position of EAS axis) at $m \geqslant 20$ was measured at zenith angles $\theta \leqslant 20$. The threshold energy of muons coming from this solid angle is 235 GeV.

In papers [3–5] we developed the method of recalculation from multiplicity spectrum to the EAS spectrum vs the total number of muons, $I(n \geqslant n_\mu)$. The formulation of the task is following: let $F(m)$ be the integral multiplicity spectrum obtained at a certain facility. Let us define the parameter $\Delta(m) = \overline{m_1}/n_\mu$, which is the average fraction of muons hitting the facility in the case when the latter is crossed by $m_1 \geqslant m$ muons. Assuming then $n_\mu = m/\Delta(m)$, we will obtain the integral spectrum of EAS vs the total number of muons

$$I(n \geqslant n_\mu) = \frac{1}{T_{rec} G(m)} F(m), \tag{I.1}$$

here $G(m)$ is the acceptance of the facility for a collection of events with muon multiplicity $\geqslant m$.

The input data and numerical values of parameters $\Delta(m)$ and $G(m)$ (calculated in [4, 5] with regard to the real structure of the facility) are presented in Table I. $N(\geqslant m)$ is the experimental number of events with the muon multiplicity $\geqslant m$ [2]. $I(n \geqslant n_\mu)$ is the integral EAS flux with the total number of muons $\geqslant n_\mu (E_\mu \geqslant 235$ GeV). The procedure of data obtaining is described in our previous paper [6].

TABLE I: Input data and numerical values of $\Delta(m)$ and $G(m)$. The error in calculation of $\Delta(m)$ and $G(m)$ does not exceed 2-3%. Non-integer values of m are obtained because of corrections at reconstruction of trajectories.

m	$N(\geqslant m)$	T_{rec}, 10^6 s	$\Delta(m)$	$G(m)$, $m^2 \cdot sr$	n_μ	$I(n \geqslant n_\mu) \times 10^7$, $(m^2 \cdot s \cdot sr)^{-1}$
32.9	547	19.33	0.289	57.9	114	4.887 ± 0.209
44.5	270	19.33	0.295	56.6	151	2.468 ± 0.150
56.5	164	19.33	0.299	54.8	189	1.548 ± 0.121
82.1	66	19.33	0.306	53.2	268	0.642 ± 0.079

*Electronic address: novoseltsev@inr.ru
†Electronic address: gveresh@gmail.com

The muon multiplicity region presented in Table I corresponds to primary energies of $10^{15} - 10^{16}$ eV. The mass composition in vicinity of the "knee" at $10^{15.5}$ eV is of special interest. This information can provide important clues to CR acceleration process and processes of formation of nuclear composition in sources of CR.

In [6] we used the same data sample to determine the mass composition averaged over the region under discussion. With the framework of three components (protons, helium and heavy nuclei) the CR mass composition in the region $10^{15} - 10^{16}$ eV was defined:

$$f_p = 0.236 \pm 0.020, \qquad f_{He} = 0.290 \pm 0.020, \qquad f_H = 0.474 \pm 0.030 \ . \tag{I.2}$$

In the present work we report the method and results which are free of previously adopted simplifications.

We try to trace the dependence of the mass composition on the energy. We assume, that the fractions of different nuclei $f_A(E)$ (E is an energy per a nucleus) are slowly changing functions of energy, and obtain quasilocal equations for differential fluxes $J_A(n_\mu)$. This allows us to extend a set of experimental data by the addition of the data on differential fluxes $J_A(n_\mu)$ and significantly refine the results of the mass composition reconstruction. At the second stage we use the smoothing procedure.

As well as in [6] we adopt the conservative scenario for the CR energy spectrum:

i) the slope change of the spectrum occurs at the same energy per unit charge $E_k(Z) = 3$ PeV$\times Z$,

ii) the spectra of all nuclei kinds have the slope exponents $\gamma_1 = 2.7$ before the "knee" and $\gamma_2 = 3.1$ after the "knee"

$$D_A(E) = I_A E^{-2.7}(1 + E/E_k(Z))^{-0.4}. \tag{I.3}$$

The paper is organized as follows.

The formal theory is developed in Section II. We find quasilocal equations for the differential EAS spectrum vs n_μ. In Section III the expected EAS spectra on n_μ (for energy spectra I.3) are calculated and the muon multiplicity n_μ is represented as a functional of the CR mass composition. In Section IV we introduce the notion of secondary experimental data and prove the smoothing procedure. In Section V the developed method is used to determine the CR mass composition in the region $0.1 - 10$ PeV. It is demonstrated that the results depend weakly on initial conditions. The dependence of average number of high energy muons on the EAS energy is discussed in Section VI. Discussion and Conclusion are presented in Section VII.

II. FORMAL THEORY

A. Formal possibilities of an exact equation

The total flux of events with the muon number $\geqslant n_\mu$ is described by means of an integral equation:

$$I_{tot}^{(exp)}(n \geqslant n_\mu) = \sum_A \int\limits_{E_{th}^{(A)}}^{\infty} f_A(E) J_A(E) P_A(E,\ n \geqslant n_\mu) dE \ , \qquad \sum_A f_A(E) = 1 \ , \tag{II.1}$$

here E is the nucleus energy, $J_A(E)$ and $f_A(E)$ are the differential flux and a fraction of nuclei with A nucleons, $P_A(E,\ n \geqslant n_\mu)$ is the probability that the number of muons (with $E_\mu \geqslant 235$ GeV) in EAS produced by nucleus "A" is $n \geqslant n_\mu$, $E_{th}^{(A)}$ is the threshold energy of nuclei with A nucleons.

We assume that the multiplicity of muons in EAS is described by the negative binomial distribution $B_A(E; n)$ (Appendix A), then

$$P_A(E,\ n \geqslant n_\mu) = \sum_{n \geq n_\mu} B_A(E,\ n)$$

According to Exp.(II.1), a contribution to the integral flux for any threshold multiplicity n_μ is formed with particles of all energies (from $E_{th}^{(A)}$ up to GZK energies). It means that on treatment of data obtained in a *limited* region of n_μ, we need to specify a mass composition model over the *whole* energy scale. For example, the most prime model is

the use of a continuous piecewise linear function of $\ln E$ with fixed boundaries of intervals $E_1,\ E_2$:

$$\begin{aligned} E_{th}^{(A)} \leqslant E \leqslant E_1 : &\qquad f_A(E) = f_A(E_{th}^{(A)}) = f_A(E_1) = \text{const} \ , \\ E_1 \leqslant E \leqslant E_2 : &\qquad f_A(E) = f_A(E_1) + C_A \ln \frac{E}{E_1} \ , \\ E \geqslant E_2 : &\qquad f_A(E) = f_A(E_1) + C_A \ln \frac{E_2}{E_1} = \text{const} \ . \end{aligned} \tag{II.2}$$

The substitution (II.2) in (II.1) gives algebraic equations for parameters $f_A(E_1),\ C_A$:

$$\begin{gathered} \sum_A \Big[f_A(E_1) \cdot I_A(n \geqslant n_\mu) + C_A \cdot \tilde{I}_A(E_1,\ E_2;\ n \geqslant n_\mu) \Big] = I_{tot}^{(exp)}(n \geqslant n_\mu) \ , \\ \sum_A f_A(E_1) = 1 \ , \qquad \sum_A C_A = 0 \ , \end{gathered} \tag{II.3}$$

where

$$\begin{aligned} I_A(n \geqslant n_\mu) &= \int\limits_{E_{th}^{(A)}}^{\infty} J_A(E) P_A(E,\ n \geqslant n_\mu) dE \ , \\ \tilde{I}_A(E_1,\ E_2;\ n \geqslant n_\mu) &= \int\limits_{E_1}^{E_2} \ln \frac{E}{E_1} \cdot J_A(E) P_A(E,\ n \geqslant n_\mu) dE + \ln \frac{E_2}{E_1} \cdot \int\limits_{E_2}^{\infty} J_A(E) P_A(E,\ n \geqslant n_\mu) dE \ . \end{aligned} \tag{II.4}$$

In the previous work [6], the equation (II.3) was the input one at $C_A = 0$ therefore there was no necessity to calculate the functions $\tilde{I}_A(E_1,\ E_2;\ n \geqslant n_\mu)$. It is impossible to generalize the results of [6] to the case $C_A \neq 0$ because the number of unknown parameters, whose values should be determined on the data (four points), is twice a large. An extension of a set of experimental data by the addition of the data on differential fluxes

$$J_{tot}^{(exp)}(n_\mu) = -\frac{\partial I_{tot}^{(exp)}}{\partial n_\mu}$$

is not succeed because the derivative from the left part of eq. (II.3) has discontinuities.

In this paper we propose a different approach based on localization of the input equation. Physically a localization possibility is ensured in that for each threshold multiplicity n_μ one can indicate a typical energy of particles (nuclei) giving a dominating contribution to integral and differential fluxes in vicinity of n_μ. In fact, the same idea is assumed in the model (II.2) that selects the energy region $E_1 \leqslant E \leqslant E_2$ which corresponds to the experimentally studied region $n_{\mu(1)} \leqslant n_\mu < n_{\mu(2)}$.

The suggested approach has two advantages in comparison with (II.3):

1) there is no necessity in concrete definition of a mass composition evolution beyond the energy region $E_1 \leqslant E \leqslant E_2$;

2) a possibility appears to extend a set of experimental data by the addition of the data on differential fluxes and, ipso facto, significantly refine the results of the mass composition reconstruction.

B. Quasilocal equations for differential fluxes

Let us turn from the equation (II.1) to a finite-difference equation:

$$\begin{gathered} \sum_A \int\limits_{E_{th}^{(A)}}^{\infty} f_A(E) J_A(E) \Delta P_A(E,\ n_\mu, n_\mu - n'_\mu) dE = \Delta I_{tot}^{(exp)}(n_\mu,\ n_\mu - n'_\mu) \ , \\ \Delta P_A(E,\ n_\mu,\ n_\mu - n'_\mu) = P_A(E,\ n \geqslant n_\mu) - P_A(E,\ n \geqslant n'_\mu) \ , \\ \Delta I_{tot}^{(exp)}(n_\mu,\ n_\mu - n'_\mu) = I_{tot}^{(exp)}(n \geqslant n_\mu) - I_{tot}^{(exp)}(n \geqslant n'_\mu) \ . \end{gathered} \tag{II.5}$$

In (II.5) n_μ is the threshold multiplicity and $n'_\mu > n_\mu$. Properties of the subintegral function permit the use of the mean value theorem:

$$\sum_A f_A[E_A(n_\mu, n_\mu - n'_\mu)] \int\limits_{E_{th}^{(A)}}^{\infty} J_A(E)\Delta P_A(E,\ n_\mu, n_\mu - n'_\mu)dE = \Delta I_{tot}^{(exp)}(n_\mu,\ n_\mu - n'_\mu)\ . \tag{II.6}$$

Here $E_A(n_\mu, n_\mu - n'_\mu)$ is an energy of nuclei with A nucleons from the energy interval which corresponds to the multiplicity region $n_\mu - n'_\mu$. On division of Eq.(II.6) by $n'_\mu - n_\mu$ and the passage to the limit $n'_\mu \to n_\mu$, we obtain the equation for a differential flux:

$$\sum_A f_A[E_A(n_\mu)]J_A(n_\mu) = J_{tot}^{(exp)}(n_\mu)\ , \tag{II.7}$$

where

$$J_{tot}^{(exp)}(n_\mu) = -\frac{\partial I_{tot}^{(exp)}(n \geqslant n_\mu)}{\partial n_\mu}\ . \tag{II.8}$$

is the differential flux of EAS vs n_μ obtained from experimental data;

$$\begin{aligned} J_A(n_\mu) &= -\frac{\partial I_A(n \geqslant n_\mu)}{\partial n_\mu}\ , \\ I_A(n \geqslant n_\mu) &= \int\limits_{E_{th}^{(A)}}^{\infty} J_A(E)P_A(E,\ n \geqslant n_\mu)dE \end{aligned} \tag{II.9}$$

are calculated differential and integral spectra. In what follows the spectra $J_A(n_\mu)$ and $I_A(n \geqslant n_\mu)$ have the status of the known functions.

Comments to the equation (II.7). It is noteworthy the value $f_A[E_A(n_\mu)]$ factored out from the integral sign depends on a form of the function $f_A(E)$ and the product $J_A(E)P_A(E,\ n \geqslant n_\mu)$ over the whole energy scale, i.e. eq. (II.7) contains a nonlocal effect implicitly. Hereafter, we shall refer to the equation (II.7) as the quasilocal one. In fact, this equation is not the one for the mass composition determination until the functions $E_A(n_\mu)$ are not realized. The situation is complicated by the fact that the functions $E_A(n_\mu)$ themselves depend on the mass composition.

The solution of listed problems in a quite good approximation can be found only for the case in which it is a priori known that $f_A(E)$ are slowly changing functions of energy.

C. Description of mass fractions $f_A(E)$ with logarithmic functions of energy

1. Equations for differential fluxes in the form of series

The exact equation (II.1) contains the products of slowly changing functions $f_A(E)$ by rapidly decreasing functions $J_A(E)$. The slowness criteria of functions $f_A(E)$ in comparison with power functions $J_A(E)$ are formulated in the form of two conditions:

1) An argument of all functions $f_A(E)$ is $\ln(E/E_0)$.

2) Starting from some order of a derivative $n > N$, derivatives of functions $f_A[\ln(E/E_0)]$ with respect to $\ln(E/E_0)$ satisfy the condition

$$\frac{1}{n!}\left(\frac{d^n f_A[\ln(E/E_0)]}{d\ln^n(E/E_0)}\right)_{E=E_0} \cdot \ln^n(E_{max}/E_0) < \mathcal{O}\left(\frac{1}{n}\right) < \frac{\varepsilon}{N}\ , \tag{II.10}$$

where $E_{\max}$ is an upper bound of field of function application; ε is a small number.

The former imposes no restrictions on generality of consideration (if the function $f_A(E)$ and its derivatives have not singularities in a domain of definition). The slowness criterion is the second condition. It is reasonable to suggest, on physical grounds, that the functions $f_A[\ln(E/E_0)]$ vary through a small range (no more than 2-3 times) in the energy range under discussion. It is well known that a slowly changing function on a bounded segment can be approximated (with a prescribed accuracy) by a finite polynomial. Note that the statement on polynomial approximation is closely

associated with the theorem of Weierstrass on the presentation of a function in the form of Taylor series; we work in practice always with a truncated series, i.e. with a polynomial.

Let us revert to the mean value theorem. The theorem states that for a given function $f_A(E)$ (and a given threshold multiplicity) there exists its average value coinciding with the value of this function at a some energy $E_A(n_\mu)$. Therefore we can write

$$\langle f_A(E)\rangle_{n_\mu} = \langle f_A[\ln(E/E_0)]\rangle_{n_\mu} = f_A\{\ln[E_A(n_\mu)/E_0]\} \ , \tag{II.11}$$

Applying Weierstrass theorem to the function $f_A(E)$, we see that the series giving the composition as a function of energy

$$f_A(E) = \sum_{k=0}^{\infty} f_{A(k)} \ln^k \frac{E}{E_0} \ , \tag{II.12}$$

corresponds to exactly the same series giving it as a function of muon multiplicity

$$f_A[E_A(n_\mu)] = \sum_{k=0}^{\infty} f_{A(k)} \ln^k \frac{E_A(n_\mu)}{E_0} \ . \tag{II.13}$$

the substitution of (II.13) in (II.7) gives:

$$\sum_A \sum_{k=0}^{\infty} f_{A(k)} \ln^k \frac{E_A(n_\mu)}{E_0} J_A(n_\mu) = J_{tot}^{(exp)}(n_\mu) \ . \tag{II.14}$$

There is one more representation of the differential spectrum equation which is mathematically equivalent to (II.14). On substitution of the series (II.12) in (II.1), the equation for integral spectrum is identically rewritten in the form:

$$\sum_A \sum_{k=0}^{\infty} f_{A(k)} I_{A(k)}(n \geqslant n_\mu) = I_{tot}^{(exp)}(n \geqslant n_\mu) \ , \tag{II.15}$$

where

$$I_{A(k)}(n \geqslant n_\mu) = \int\limits_{E_{th}^{(A)}}^{\infty} \ln^k \frac{E}{E_0} \cdot J_A(E) P_A(E, \ n \geqslant n_\mu) dE \tag{II.16}$$

are "coefficients of order k" at $f_{A(k)}$ which are determined by direct calculations (below we shall also name them "calculated spectra of the k-th order").

The equation for differential spectrum is obtained by differentiation of equation (II.15):

$$-\sum_A \sum_{k=0}^{\infty} f_{A(k)} \frac{\partial I_{A(k)}}{\partial n_\mu} = J_{tot}^{(exp)}(n_\mu) \ . \tag{II.17}$$

Equations (II.14) and (II.17) are mathematically equivalent if Weierstrass theorem is true for the function $f_A(E)$ and the function $J(E)$ becomes zero at some energy $E = E_{max}$ (at GZK energies). The two conditions are fulfilled. It is plain, that this equivalence, in a mathematical sense, has place only when infinite series in (II.14) and (II.17) are taken into consideration in full. Identifying series in (II.14) and (II.17), we get nonlocal equations for functions $E_A(n_\mu)$:

$$\sum_{k=1}^{\infty} f_{A(k)} \left[\frac{\partial I_{A(k)}}{\partial n_\mu} + \ln^k \frac{E_A(n_\mu)}{E_0} \cdot J_A(n_\mu) \right] = 0 \ . \tag{II.18}$$

It should be stressed that until now no approximations and mass composition models are used. A choice of $f(\ln(E/E_0))$ representation restricts in no way of consideration generality; it has been done for convenience in operation.

2. Approximations and the finding of functions $E_A(n_\mu)$

Approximations, which are listed below, pursue two goals
1) to realize functions $E_A(n_\mu)$,
2) to convert the quasilocal equation (II.7) (or its representation in the form of the series (II.14)) in a local equation describing the differential flux in a comparatively narrow interval of muon multiplicities.

As mentioned earlier, the functions $E_A(n_\mu)$ depend on both the nuclei fractions $f_A(E)$ (i.e., from k-order corrections $f_{A(k)}$ in exp. (II.12)) and the product

$$\Gamma_A(E,\ n_\mu) = J_A(E) \cdot P_A(E,\ n \geqslant n_\mu).$$

Let us adopt two simplifying assumptions:
1) In the case of slowly changing functions $f_A(E)$ with energy (i.e. in case of functions $E_A(n_\mu)$ are under the logarithm sign), the functional dependence of $E_A(n_\mu)$ on the mass composition can be ignored. In what follows, it is assumed that deviation of $f_A[E_A(n_\mu)]$ from constants is defined only by subintegral functions $\Gamma_A(E,\ n_\mu)$. This assumption means the independence of $E_A(n_\mu)$ from $f_{A(k\geqslant 1)}$. In this case the equation (II.18) is converted to the equation system

$$-\frac{\partial I_{A(k)}}{\partial n_\mu} = \ln^k \frac{E_A(n_\mu)}{E_0} \cdot J_A(n_\mu)\ , \qquad k = 1,\ 2,\ 3,\ \ldots\ . \tag{II.19}$$

2) The second simplifying assumption is the slowness condition of the mass composition evolution with energy: we assume that functions $f_A[\ln(E/E_0)]$ satisfy the inequalities (II.10). In this case the infinite equation system (II.19) is transform to a finite system: $k = 1,\ 2,\ \ldots,\ N$.

Within the framework accepted assumptions the functions $E_A(n_\mu)$ do not depend on the composition evolution with energy, but they depend only on the degree of slowness of this evolution – the latter is given by fixing $k_{max} = N$ in (II.19).

An algorithm of determining functions $E_A(n_\mu)$ is based on numerical calculations with the help of expressions (II.16) with subsequent matching of analytical approximations for results of these calculations. For coefficients of zero and the first orders, the simplest approximations are

$$I_{A(0)}(n \geqslant n_\mu) = I_{n_0}^{(A)} \left(\frac{n_0}{n_\mu}\right)^{\beta_A}\ , \qquad I_{A(1)}(n \geqslant n_\mu) = I_{n_0}^{(A)} \left(\frac{n_0}{n_\mu}\right)^{\beta_A} \ln\left(\frac{n_\mu}{\tilde{n}_A(E_0)}\right)^{\alpha_A}\ . \tag{II.20}$$

Here n_0 is an arbitrary normalization multiplicity (for example $n_0 = 114$); $I_{n_0}^{(A)},\ \beta_A,\ \tilde{n}_A(E_0),\ \alpha_A$ are parameters whose values are adjusted by fitting calculated data. Next we calculate derivatives

$$\begin{gathered} J_A(n_\mu) = -\frac{\partial I_{A(0)}}{\partial n_\mu} = I_{n_0}^{(A)} \frac{\beta_A}{n_0} \left(\frac{n_0}{n_\mu}\right)^{\beta_A+1}\ , \\ -\frac{\partial I_{A(1)}}{\partial n_\mu} = I_{n_0}^{(A)} \frac{\beta_A}{n_0} \left(\frac{n_0}{n_\mu}\right)^{\beta_A+1} \ln\left(\frac{n_\mu}{n_A(E_0)}\right)^{\alpha_A}\ , \\ n_A(E_0) = \tilde{n}_A(E_0) e^{1/\beta_A}\ . \end{gathered} \tag{II.21}$$

Formulas (II.21) are substituted in the first equation (II.19) (at $k = 1$), following which an expression for $E_A(n_\mu)$ results:

$$E_A(n_\mu) = E_0 \cdot \left(\frac{n_\mu}{n_A(E_0)}\right)^{\alpha_A}\ . \tag{II.22}$$

Note the inverse dependence is

$$n_\mu^{(A)}(E) = n_A(E_0) \cdot \left(\frac{E}{E_0}\right)^{\zeta_A}\ , \qquad \zeta_A = \frac{1}{\alpha_A}\ . \tag{II.23}$$

Thus the approximations (II.20) correspond to the assumption on the power dependence of muon multiplicity from a nucleus energy. Note that exponents ζ_A are different for different nuclei. It is plain, the characteristic multiplicity

$n_\mu^{(A)}(E)$ calculated according to (II.23) coincides with the average multiplicity with an accuracy up to multiplicative coefficient of the order of the unity. Later on, we show this by direct calculations.

We return to equations (II.19). With the use of approximations (II.20) and exp. (II.22) these equations can be integrated. The resultant expressions are:

$$I_{A(k)}(n \geqslant n_\mu) = I_{n_0}^{(A)} \left(\frac{n_0}{n_\mu}\right)^{\beta_A} k! \left(\frac{\alpha_A}{\beta_A}\right)^k \sum_{m=0}^{k} \frac{\beta_A^m}{m!} \ln^m \frac{n_\mu}{n_A(E_0)} , \qquad k = 0,\ 1,\ 2,\ \ldots . \tag{II.24}$$

$$J_{A(k)}(n_\mu) = \frac{\beta_A I_{n_0}^{(A)}}{n_0} \left(\frac{n_0}{n_\mu}\right)^{\beta_A+1} \alpha_A^k \ln^k \frac{n_\mu}{n_A(E_0)} , \qquad k = 0,\ 1,\ 2,\ \ldots . \tag{II.25}$$

If necessary, approximations (II.20) can be refined. Let us suppose that experimental data point at a change in the slope exponent β with a rise in n_μ (such a situation is not precluded because the energy spectrum has the break). In this case the coefficients of zero and the first orders are approximated by expressions

$$\begin{aligned} I_{A(0)}(n \geqslant n_\mu) &= I_{n_0}^{(A)} \left(\frac{n_0}{\varphi_A(n_\mu)}\right)^{\beta_A} , \\ I_{A(1)}(n \geqslant n_\mu) &= I_{n_0}^{(A)} \left(\frac{n_0}{\varphi_A(n_\mu)}\right)^{\beta_A} \ln \left(\frac{\varphi_A(n_\mu)}{\tilde{n}_A(E_0)}\right)^{\alpha_A} \end{aligned} \tag{II.26}$$

where

$$\varphi_A(n_\mu) = n_\mu \left[1 + \kappa_A \left(\frac{n_\mu}{n_A(E_0)}\right)^{\alpha_A}\right]^{1/\alpha_A} , \tag{II.27}$$

κ_A is new parameter. Instead of (II.27), it can be chosen other function; the choice depends on a multiplicity interval under investigation. The differential spectra have the appearance

$$\begin{aligned} J_A(n_\mu) &= -\frac{\partial I_{A(0)}}{\partial n_\mu} = \frac{\beta_A I_{n_0}^{(A)}}{n_0} \left(\frac{n_0}{\varphi_A(n_\mu)}\right)^{\beta_A+1} \varphi'_A(n_\mu) , \\ -\frac{\partial I_{A(1)}}{\partial n_\mu} &= \frac{\beta_A I_{n_0}^{(A)}}{n_0} \left(\frac{n_0}{\varphi_A(n_\mu)}\right)^{\beta_A+1} \varphi'_A(n_\mu) \ln \left(\frac{\varphi_A(n_\mu)}{n_A(E_0)}\right)^{\alpha_A} , \\ n_A(E_0) &= \tilde{n}_A(E_0) e^{1/\beta_A} . \end{aligned} \tag{II.28}$$

where $\varphi'_A(n_\mu) = d\varphi_A/dn_\mu$. Substitution of expressions (II.26), (II.27) in the first equation from (II.19) gives the refined formula for $E_A(n_\mu)$:

$$E_A(n_\mu) = E_0 \cdot \left(\frac{\varphi_A(n_\mu)}{n_A(E_0)}\right)^{\alpha_A} . \tag{II.29}$$

Note that on substitution of (II.27) in (II.19) any one of equations (II.21) is rewritten in the form

$$-\frac{\partial I_{A(k)}}{\partial \varphi_A(n_\mu)} = \frac{\beta_A I_{n_0}^{(A)}}{n_0} \left(\frac{n_0}{\varphi_A(n_\mu)}\right)^{\beta_A+1} \cdot \alpha^k \ln^k \frac{\varphi_A(n_\mu)}{n_A(E_0)} , \qquad k = 1,\ 2,\ 3,\ \ldots . \tag{II.30}$$

Upon integrating the equations (II.30) we obtain

$$I_{A(k)}(n \geqslant n_\mu) = I_{n_0}^{(A)} \left(\frac{n_0}{\varphi_A(n_\mu)}\right)^{\beta_A} k! \left(\frac{\alpha_A}{\beta_A}\right)^k \sum_{m=0}^{k} \frac{\beta_A^m}{m!} \ln^m \frac{\varphi_A(n_\mu)}{n_A(E_0)} , \qquad k = 0,\ 1,\ 2,\ \ldots . \tag{II.31}$$

$$\begin{aligned} J_{A(k)}(n_\mu) &= -\frac{\partial I_{A(k)}}{\partial n_\mu} = J_A(n_\mu) \ln^k \left(\frac{\varphi_A(n_\mu)}{n_A(E_0)}\right)^{\alpha_A} = \\ &= \frac{\beta_A I_{n_0}^{(A)}}{n_0} \left(\frac{n_0}{\varphi_A(n_\mu)}\right)^{\beta_A+1} \varphi'_A(n_\mu) \alpha_A^k \ln^k \frac{\varphi_A(n_\mu)}{n_A(E_0)} , \qquad k = 0,\ 1,\ 2,\ \ldots . \end{aligned} \tag{II.32}$$

D. Quasilocal equations for the EAS spectrum vs n_μ

Quasilocal equations are obtained by substituting (II.31) in (II.15) (for the integral spectrum) and (II.32) in (II.14) (for the differential spectrum):

$$\sum_A I_{n0}^{(A)} \left(\frac{n_0}{\varphi_A(n_\mu)}\right)^{\beta_A} \sum_{k=0}^{N} f_{A(k)} k! \left(\frac{\alpha_A}{\beta_A}\right)^k \sum_{m=0}^{k} \frac{\beta_A^m}{m!} \ln^m \frac{\varphi_A(n_\mu)}{n_A(E_0)} = I_{tot}^{(exp)}(n \geqslant n_\mu) \ , \tag{II.33}$$

$$\sum_A \frac{\beta_A I_{n0}^{(A)}}{n_0} \left(\frac{n_0}{\varphi_A(n_\mu)}\right)^{\beta_A+1} \varphi'_A(n_\mu) \sum_{k=0}^{N} f_{A(k)} \alpha_A^k \ln^k \frac{\varphi_A(n_\mu)}{n_A(E_0)} = J_{tot}^{(exp)}(n_\mu) \ . \tag{II.34}$$

In (II.33), (II.34) unknown variables are $f_{A(k)}$ — the coefficients in polynomials of the order N:

$$\begin{gathered} f_A(E) = f_{A(0)} + \sum_{k=1}^{N} f_{A(k)} \ln^k \frac{E}{E_0} \ , \\ \sum_A f_{A(0)} = 1 \ , \qquad \sum_A f_{A(k)} = 0 \ , \qquad k = 1,\ 2,\ ...,\ N \ . \end{gathered} \tag{II.35}$$

We enumerate once more all assumptions used to yield the equations (II.33), (II.34).

1) The nuclei fractions are slow functions of energy $f_A[\ln(E/E_0)]$ whose derivatives satisfy the condition (II.10).

2) Energies $E_A(n_\mu)$ arising in the mean value theorem do not depend on the evolution of variables f_A with energy.

3) The integral calculated spectra of zero and the first orders are assumed to be approximated by expressions (II.26).

The first assumption reflects most likely those properties of functions $f_A(E)$ which they have in actuality. The second assumption holds so much the better, the slower are functions $f_A(E)$. As regards the third assumption, it affects in no way on the estimate of theory capabilities. It is plain, that approximations (II.26) with matching a function $\varphi_A(n_\mu)$ can reproduce calculations from the formula (II.16) with given in advance accuracy.

Physically the smallness of nonlocal effects is ensured by the rapid power decrease of CR energy spectrum and a slow evolution of functions $f_A(E)$. A weak trace of nonlocality is contained in calculated spectra $I_{A(k)}(n \geqslant n_\mu)$.

III. CALCULATED SPECTRA

A. Results of calculations and approximations

We have experimental data obtained on the rather narrow interval of muon multiplicity. Therefore the simplest approximations (II.24), (II.25) will be used below. Parameters of calculated spectra approximations are established by means of fitting results of calculations of coefficients $I_{A(k)}(n \geqslant n_\mu)$ $(k = 0, 1, 2)$. Obtained below the values of parameters $I_{n0}^{(A)},\ \beta_A,\ n_A(E_0),\ \alpha_A$ can be refined with regard of computation results of top order coefficients.

The results of calculations of zero, first and second orders coefficients are presented in lines "n_μ-calc" of Table II. The calculations are performed from the formulae (II.16) with $E_0 = 0.1$ PeV. According to (II.16) one can always pass to an other value of E'_0:

$$\begin{gathered} I_{A(1)}(E'_0,\ n \geqslant n_\mu) = I_{A(1)}(E_0,\ n \geqslant n_\mu) + \left(\ln \frac{E_0}{E'_0}\right) \cdot I_{A(0)}(n \geqslant n_\mu) \ , \\ I_{A(2)}(E'_0,\ n \geqslant n_\mu) = I_{A(2)}(E_0,\ n \geqslant n_\mu) + 2\left(\ln \frac{E_0}{E'_0}\right) \cdot I_{A(1)}(n \geqslant n_\mu) + \left(\ln^2 \frac{E_0}{E'_0}\right) \cdot I_{A(0)}(n \geqslant n_\mu) \ . \end{gathered} \tag{III.1}$$

We adopt (as in [6]) the total flux of nuclei with energy of $E = 100$ TeV is equal to $J_{tot}(100\ \text{TeV}) = 11.8 \times 10^{-10} (\text{m}^2 \cdot \text{s} \cdot \text{sr} \cdot\ \text{GeV})^{-1}$ according to the result obtained at the Tibet array [7]. A statistical uncertainty of the total flux is taken into consideration by a factor $1 + \Delta$, where $-0.1 < \Delta < 0.1$.

TABLE II: The results of calculations and approximations of calculated spectra (all values are multiplied by 10^7)

n_μ	$I_{p(0)}$	$I_{p(1)}$	$I_{p(2)}$	$I_{He(0)}$	$I_{He(1)}$	$I_{He(2)}$	$I_{N(0)}$	$I_{N(1)}$	$I_{N(2)}$	$I_{Si(0)}$	$I_{Si(1)}$	$I_{Si(2)}$	$I_{Fe(0)}$	$I_{Fe(1)}$	$I_{Fe(2)}$
114-calc	1.199	4.697	18.775	2.766	9.966	36.772	5.609	18.676	64.037	7.616	24.275	79.958	9.432	29.072	92.84
114-appr	1.206	4.727	18.84	2.785	10.039	36.943	5.64	18.78	64.281	7.667	24.419	80.277	9.538	29.326	93.393
151-calc	0.583	2.497	10.877	1.397	5.538	22.376	2.98	10.985	41.443	4.166	14.728	53.439	5.392	18.378	64.449
151-appr	0.579	2.485	10.814	1.389	5.51	22.244	2.967	10.94	41.253	4.145	14.657	53.186	5.345	18.235	64.013
189-calc	0.323	1.482	6.894	0.802	3.414	14.757	1.787	7.096	28.73	2.552	9.737	37.97	3.401	12.501	47.071
189-appr	0.322	1.479	6.868	0.797	3.392	14.663	1.777	7.058	28.582	2.536	9.68	37.777	3.366	12.389	46.732
268-calc	0.129	0.651	3.322	0.334	1.572	7.485	0.797	3.518	15.758	1.176	5.00	21.631	1.627	6.67	27.87
268-appr	0.129	0.654	3.337	0.336	1.58	7.535	0.80	3.533	15.846	1.181	5.024	21.754	1.639	6.719	28.094

The spectra, calculated from the formulae (II.16), are approximated by expressions

$$I_{A(0)}(n \geqslant n_\mu) = (1+\Delta) I_{114}^{(A)} \left(\frac{114}{n_\mu}\right)^{\beta_A} ,$$

$$I_{A(1)}(n \geqslant n_\mu) = (1+\Delta) I_{114}^{(A)} \left(\frac{114}{n_\mu}\right)^{\beta_A} \left[\ln\left(\frac{n_\mu}{n_A(E_0)}\right)^{\alpha_A} + \frac{\alpha_A}{\beta_A}\right] , \qquad \text{(III.2)}$$

$$I_{A(2)}(n \geqslant n_\mu) = (1+\Delta) I_{114}^{(A)} \left(\frac{114}{n_\mu}\right)^{\beta_A} \left[\ln^2\left(\frac{n_\mu}{n_A(E_0)}\right)^{\alpha_A} + 2\frac{\alpha_A}{\beta_A}\ln\left(\frac{n_\mu}{n_A(E_0)}\right)^{\alpha_A} + \frac{2\alpha_A^2}{\beta_A^2}\right] .$$

The values of parameters $I_{n_0}^{(A)},\ \beta_A,\ n_A(E_0),\ \alpha_A$ are listed in the Table III. By comparison we present two sets of parameters values, one of which is obtained in a quadratic model with the aid of joint fitting three coefficients $I_{A(0)},\ I_{A(1)},\ I_{A(2)}$ and the second is obtained with two coefficients $I_{A(0)},\ I_{A(1)}$ (a linear model). As is seen from the table, there is good reason to believe that the dependence on the number of fitted spectra $I_{A(k)}$ is weak. The results of the calculations from the formulae (III.2), corresponding to joint fitting three coefficients, are presented in lines "n_μ-appr" of the table II. The relative error of approximations is less than 1 %.

Note the values of $I_{114}^{(A)},\ \beta_A,\ \alpha_A$ do not depend on the choice of the energy E_0. In passing to another normalization energy E_0' according to formulae (III.1), the parameter $n_A(E_0)$ rearranges as follows $n_A(E_0')$:

$$n_A(E_0) \longrightarrow n_A(E_0') = n_A(E_0) \cdot \left(\frac{E_0'}{E_0}\right)^{\zeta_A} . \qquad \text{(III.3)}$$

The values of parameters $\zeta_A = 1/\alpha_A$ are listed in the last lines of the Table III.

Upon differentiation of expressions (III.2) we get:

$$-\frac{\partial I_{A(0)}}{\partial n_\mu} = J_A(n_\mu) = (1+\Delta)\frac{\beta_A}{114} I_{114}^{(A)} \left(\frac{114}{n_\mu}\right)^{\beta_A+1} ,$$

$$-\frac{\partial I_{A(1)}}{\partial n_\mu} = (1+\Delta)\frac{\beta_A}{114} I_{114}^{(A)} \left(\frac{114}{n_\mu}\right)^{\beta_A+1} \ln\left(\frac{n_\mu}{n_A(E_0)}\right)^{\alpha_A} , \qquad \text{(III.4)}$$

$$-\frac{\partial I_{A(2)}}{\partial n_\mu} = (1+\Delta)\frac{\beta_A}{114} I_{114}^{(A)} \left(\frac{114}{n_\mu}\right)^{\beta_A+1} \ln^2\left(\frac{n_\mu}{n_A(E_0)}\right)^{\alpha_A} .$$

TABLE III: Approximation parameters of calculated spectra

	p	He	N	Si	Fe	Fit
$I_{114}^{(A)}$	1.206	2.785	5.640	7.667	9.538	$I_{A(0)},\ I_{A(1)},\ I_{A(2)}$
$I_{114}^{(A)}$	1.207	2.788	5.644	7.672	9.543	$I_{A(0)},\ I_{A(1)}$
β_A	2.611	2.476	2.285	2.188	2.060	$I_{A(0)},\ I_{A(1)},\ I_{A(2)}$
β_A	2.612	2.477	2.286	2.190	2.062	$I_{A(0)},\ I_{A(1)}$
α_A	1.325	1.293	1.270	1.250	1.198	$I_{A(0)},\ I_{A(1)},\ I_{A(2)}$
α_A	1.332	1.301	1.278	1.255	1.198	$I_{A(0)},\ I_{A(1)}$
$n_A(E_0)$	8.673	10.516	12.821	14.088	14.223	$I_{A(0)},\ I_{A(1)},\ I_{A(2)}$
$n_A(E_0)$	8.868	10.738	13.068	14.081	14.206	$I_{A(0)},\ I_{A(1)}$
$\zeta_A = 1/\alpha_A$	0.755	0.773	0.787	0.80	0.835	$I_{A(0)},\ I_{A(1)},\ I_{A(2)}$
$\zeta_A = 1/\alpha_A$	0.751	0.769	0.782	0.797	0.835	$I_{A(0)},\ I_{A(1)}$

The substitution of (III.4) in (II.19) at $k = 1$ leads to the equation for $E_A(n_\mu)$:

$$E_A(n_\mu) = E_0 \cdot \left(\frac{n_\mu}{n_A(E_0)}\right)^{\alpha_A} . \tag{III.5}$$

The expression (III.5) is the relation between a multiplicity scale of high energy muons and an energy scale of nuclei (with A nucleons) which produced these muons. The dependence $E_A(n_\mu)$ for the multiplicity interval under discussion $114 \leqslant n_\mu \leqslant 268$ is shown in the table IV.

B. Determining the mass composition on the base of the dependence $n_\mu(E)$

The energy $E_A(n_\mu)$ in (III.5) is slightly different from the average energy $\overline{E}_A(n_\mu)$ of nuclei producing the same number of muons. The point is the formula for $E_A(n_\mu)$ is obtained from the expression for an average value of the logarithm of energy, which, in general, does not coincide with the logarithm of an average energy. However by virtue of the slowness of the logarithmic function, a difference between $E_A(n_\mu)$ and $\overline{E}_A(n_\mu)$ has to be small. If this difference can be neglected, then the inverse function to (III.5) gives the dependence of the average number of high energy muons produced by a nucleus "A" on the energy of this nucleus:

$$n_\mu^{(A)}(E) = n_A(E_0) \cdot \left(\frac{E}{E_0}\right)^{\zeta_A} . \tag{III.6}$$

The formulae (III.6) allow us to represent the muon multiplicity n_μ as a functional of the CR mass composition. Certainly, it should be taken into account that the same number of muons are produced by different nuclei with different energies:

$$n_\mu = \sum_A f_A[E_A(n_\mu)] \cdot n_\mu^{(A)}[E_A(n_\mu)] . \tag{III.7}$$

If the mass composition is established properly, then plugging numbers from the table IV in (III.7) we have to get the identities. We shall return to this question in Section VI.

TABLE IV: Relationships between the nuclei energies scale (E in PeV) and the muon multiplicity scale

n_μ	E_p	E_{He}	E_N	E_{Si}	E_{Fe}
114	3.028	2.176	1.600	1.363	1.208
131	3.649	2.611	1.913	1.625	1.430
147	4.236	3.020	2.207	1.870	1.636
151	4.397	3.132	2.287	1.937	1.692
169	5.104	3.623	2.639	2.230	1.937
175	5.343	3.789	2.757	2.329	2.019
189	5.925	4.191	3.045	2.567	2.217
201	6.438	4.545	3.297	2.776	2.389
225	7.474	5.257	3.803	3.196	2.734
268	9.428	6.595	4.751	3.979	3.373

IV. EXPERIMENTAL DATA

A. Primary and secondary data

Four experimental points of the integral EAS spectrum are fitted with a high enough accuracy by a power function

$$I_{tot}^{(exp)}(n \geqslant n_\mu) = I_{114}^{(A)} \cdot \left(\frac{114}{n_\mu}\right)^{\beta} \ . \tag{IV.1}$$

$$I_{114}^{(A)} = (4.873 \pm 0.194) \cdot 10^{-7} (\mathrm{m}^2 \cdot \mathrm{s} \cdot \mathrm{sr})^{-1} \ , \qquad \beta = 2.344 \pm 0.122 \ , \qquad \chi^2/dof = 0.199 \ . \tag{IV.2}$$

Deviations of the fitting curve from experimental points exceed nowhere of a half of statistical error. The latter means that the smoothing of experimental data within the limits of a half-width of error band allows us to get an ideal agreement of smoothed-out data with the fitting curve. Moreover, the smoothing procedure can be performed by means of data correction within the limits of small systematic errors associated with Monte-Carlo calculations of magnitudes $\Delta(m)$ and $G(m)$.

In cases when a power interpolation (IV.1) stays within a half of error band, there is an algorithm of a decrease of fitted parameters uncertainties: experimental data are written in the logarithmic variables, i.e. the integral flux logarithm is considered as a function of the multiplicity logarithm. Next, by means of enumeration of all possible pairs of experimental points, three sets out of the six points are calculated:

$$-\beta(\ln n_\mu) = \frac{\ln\left(I_{tot}^{(exp)}(n \geqslant n''_\mu)\right) - \ln\left(\cdot I_{tot}^{(exp)}(n \geqslant n'_\mu)\right)}{\ln n''_\mu - \ln n'_\mu} \ , \tag{IV.3}$$

$$\ln\left(\tilde{I}_{tot}^{(exp)}(n \geqslant n_\mu)\right) = \frac{1}{2}\left[\ln\left(I_{tot}^{(exp)}(n \geqslant n''_\mu)\right) + \ln\left(I_{tot}^{(exp)}(n \geqslant n'_\mu)\right)\right] \ . \tag{IV.4}$$

$$\ln\left(\tilde{J}_{tot}^{(exp)}(n_\mu)\right) = \ln\left(\beta(\ln n_\mu)\right) - \ln n_\mu + \ln\left(\tilde{I}_{tot}^{(exp)}(n \geqslant n_\mu)\right) \ . \tag{IV.5}$$

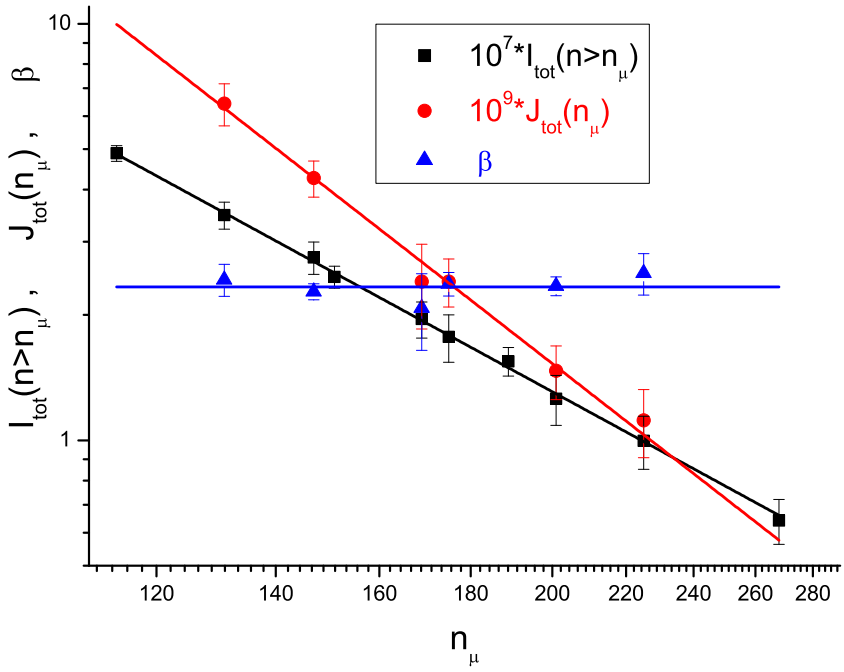

FIG. 1: The EAS spectrum vs n_μ and the spectrum slope exponent data. Numerical values of integral fluxes $I_{tot}^{(exp)}(n \geqslant n_\mu)$, differential fluxes $J_{tot}^{(exp)}(n_\mu)$ and the spectrum slope exponent β are listed in the table V. The fit of data was carried out from the formulae (IV.7). The results are presented in (IV.8).

Each of sets gains the status of a function of a variable

$$\ln n_\mu = \frac{1}{2}\left(\ln n''_\mu + \ln n'_\mu\right) \ .$$

Now we read the mathematical criterion the fulfillment of which gives an additional confirmation of the power spectrum. According to (IV.1) the integral flux logarithm is *a linear* function of the multiplicity logarithm:

$$\ln\left(I_{tot}^{(exp)}(n \geqslant n_\mu)\right) = \ln\left(\frac{I_{114}^{(A)}}{114^\beta}\right) - \beta \ln n_\mu \ . \qquad \text{(IV.6)}$$

As is known, a linear function possesses two unique properties:

1) its derivative is constant and is exactly equal to the ratio of finite differences (calculated for any two points belonging to this function);

2) the arithmetic mean of two values of a linear function belongs to the same function in the point which is the arithmetic mean of two arguments.

Therefore the criterion is stated as follows:

The input data after taking the logarithm belong to the linear function (IV.6), if within the limits of measurement errors 1) all numbers of the set (IV.3) coincide; 2) all values (IV.4) belong to the same function; 3) the sum of functions in the right part of (IV.5) is a linear function.

The numbers (IV.3) and exponents from numbers (IV.4), (IV.5) together with the input data are listed in the table V and plot in Fig.1. It is not too difficult to see from Fig.1 that, within the measurement error limits, the linearity criteria are fulfilled for both the integral and differential spectra, including the condition of the spectrum

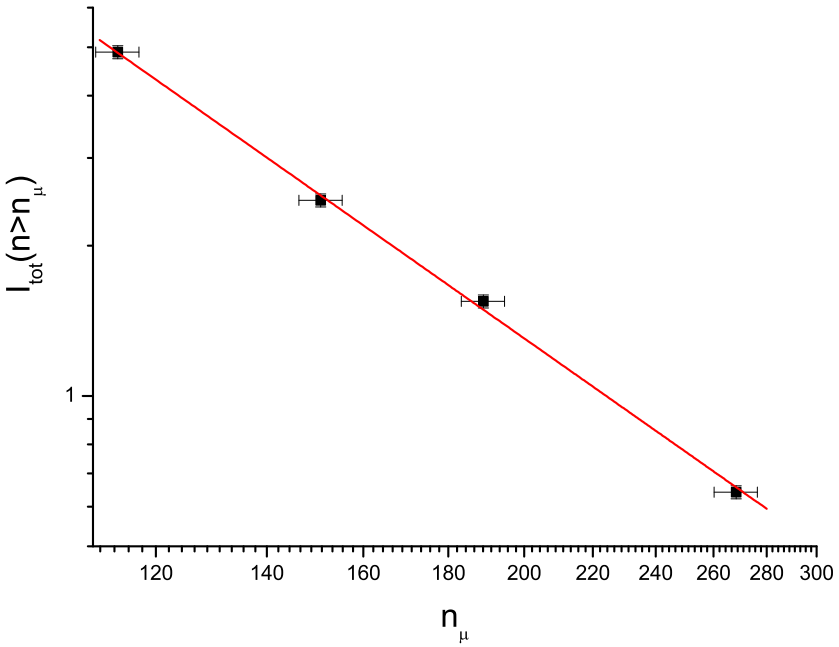

FIG. 2: The integral EAS spectrum vs n_μ with systematic errors related to the calculation of $\Delta(m)$ and $G(m)$. Fitting curve is constructed from the first formula (IV.7) with parameters (IV.8).

TABLE V: Primary and secondary experimental data on the EAS spectrum vs $n_\mu(E_\mu \geqslant 235$ GeV)

n_μ	$I_{tot}^{(exp)}(n \geqslant n_\mu)$, $10^7(\mathrm{m}^2\cdot\mathrm{s}\cdot\ \mathrm{sr})^{-1}$	$J_{tot}^{(exp)}(n_\mu)$, $10^9(\mathrm{m}^2\cdot\mathrm{s}\cdot\ \mathrm{sr})^{-1}$	β
114	4.887 ± 0.209	–	–
131	3.473 ± 0.258	6.434 ± 0.741	2.431 ± 0.214
147	2.750 ± 0.245	4.261 ± 0.424	2.274 ± 0.101
151	2.468 ± 0.150	–	–
169	1.955 ± 0.194	2.404 ± 0.554	2.078 ± 0.433
175	1.771 ± 0.231	2.406 ± 0.318	2.375 ± 0.153
189	1.548 ± 0.121	–	–
201	1.259 ± 0.173	1.469 ± 0.216	2.347 ± 0.122
225	0.997 ± 0.145	1.116 ± 0.207	2.520 ± 0.289
268	0.642 ± 0.079	–	–

slope constancy. The joint fit of three data sets presented in the table V has been performed from the formulae

$$I_{tot}^{(exp)}(n \geqslant n_\mu) = I_{114}^{(A)} \cdot \left(\frac{114}{n_\mu}\right)^{\beta} ,$$
$$J_{tot}^{(exp)}(n_\mu) = -\frac{\partial I_{tot}^{(exp)}(n \geqslant n_\mu)}{\partial n_\mu} = \frac{\beta}{114} I_{114}^{(A)} \cdot \left(\frac{114}{n_\mu}\right)^{\beta+1} , \qquad \text{(IV.7)}$$
$$\beta(n_\mu) = \beta .$$

The following values of fitted parameters have been obtained:

$$I_{114}^{(A)} = (4.855 \pm 0.103) \cdot 10^{-7} (\mathrm{m}^2 \cdot \mathrm{s} \cdot \mathrm{sr})^{-1} , \qquad \beta = 2.337 \pm 0.056 , \qquad \chi^2/dof = 0.115 . \qquad \text{(IV.8)}$$

Let us emphasize once again: the fact that the results of calculations from the formulae (IV.3) — (IV.5) are reproduced by functions (IV.7) with parameters (IV.8) is not in advance assumed and is no general considerations guaranteed. The possibility of a such description arises only because the spectrum is indeed of power type with high accuracy, while precision of four experimental points $I_{tot}^{(exp)}(n \geqslant n_\mu)$ is sufficient for determining parameters of the spectrum.

B. The smoothing procedure

As mentioned earlier, the values of $\Delta(m)$, $G(m)$ have the errors $\simeq$ 2-3%. These errors induce *systematic* errors in the values n_μ and $I_{tot}^{(exp)}(n \geqslant n_\mu)$. (Above these errors did not take into account). Primary experimental data with regard to only systematic errors are presented in Fig.2. The solid line shows the fitting curve constructed from the first formula of (IV.7). We use in this formula the same parameters (IV.8) obtained by joint fit of primary and secondary experimental data. As is seen from Fig.2 inside of rectangles generated by systematic errors there are the points belonging to the fitting curve. Thus both statistical and systematic errors in the region $114 \leqslant n_\mu \leqslant 268$ allow to use no spectrum variants other than a simplest two-parameter power spectrum. (A spectrum having more than two parameters will lead to an over-fitting.)

Smoothed-out experimental data are identified with the values of the fitting function and are specified in each integer-valued point of the muon multiplicity interval $114 \leqslant n_\mu \leqslant 268$. The error values are also interpolated and given in the same points. In this way constructed smoothed-out data are presented in Fig.5. The joint fit of these data from the formulae (IV.7) cannot certainly lead to the values of fitted parameters different from (IV.7). Smoothed-out data will be used in the Section V D.

V. THE CR MASS COMPOSITION IN THE ENERGY REGION 1 — 10 PEV

A. Requirements to the mass composition model

In this Section we use the developed formalism to the same data as in [6] to compare the results with the ones obtained in [6].

A quasilocal nature of the equations has the key importance for finding PCR mass composition. Quasilocal equations allows us to work in each ¡¡piece¿¿ individually sewing results obtained in neighboring pieces. A piecewise quadratic function is continuous after linkage together with the first derivative.

As is seen from the table IV, the multiplicity region $114 \leqslant n_\mu \leqslant 268$ corresponds to the energy region 1 PeV $\leqslant E \leqslant$ 10 PeV. In this region we choose the approximations of calculated spectra $I_{A(k)}$ in the form (II.24), (II.25) with the parameter $n_0 = 114$. The values of parameters $I_{114}^{(A)}$, β_A, α_A, $n_A(E_0)$ are listed in the table III. (We use the parameters obtained by joint fit of three calculated spectra $I_{A(0)}$, $I_{A(1)}$, $I_{A(2)}$.) Equations for the integral and differential spectra take now the form:

$$(1+\Delta) \sum_A I_{114}^{(A)} \left(\frac{114}{n_\mu}\right)^{\beta_A} \sum_{k=0}^{N_{appr}} f_{A(k)} k! \left(\frac{\alpha_A}{\beta_A}\right)^k \sum_{m=0}^{k} \frac{\beta_A^m}{m!} \ln^m \frac{n_\mu}{n_A(E_0)} = I_{tot}^{(exp)}(n \geqslant n_\mu) , \qquad \text{(V.1)}$$

$$(1+\Delta) \sum_A \frac{\beta_A I_{114}^{(A)}}{114} \left(\frac{114}{n_\mu}\right)^{\beta_A+1} \sum_{k=0}^{N_{appr}} f_{A(k)} \alpha_A^k \ln^k \frac{n_\mu}{n_A(E_0)} = J_{tot}^{(exp)}(n_\mu) . \qquad \text{(V.2)}$$

Taking into account that formulae (V.1), (V.2) are meant for the reproduction of the power spectrum, we introduce one more fitting function for the spectrum slope exponent:

$$\frac{\sum\limits_A \beta_A I_{114}^{(A)} \left(\frac{114}{n_\mu}\right)^{\beta_A} \sum\limits_{k=0}^{N_{appr}} f_{A(k)} \alpha_A^k \ln^k \frac{n_\mu}{n_A(E_0)}}{\sum\limits_A I_{114}^{(A)} \left(\frac{114}{n_\mu}\right)^{\beta_A} \sum\limits_{k=0}^{N_{appr}} f_{A(k)} k! \left(\frac{\alpha_A}{\beta_A}\right)^k \sum\limits_{m=0}^{k} \frac{\beta_A^m}{m!} \ln^m \frac{n_\mu}{n_A(E_0)}} = \beta(n_\mu) \ . \tag{V.3}$$

A polynomial order N_{appr} is fixed by the choice of an evolution model of the mass composition in the energy interval under discussion.

As initial conditions we use at first the same "composition Swordy" at $E_0' = 0.1$ PeV that we used in [6] (to compare the present results with the ones in [6])

	p	He	CNO	Ne-S	Fe
A	1	4	14	28	56
$f, \%$	25	31	19	12	13

(V.4)

and then consider more "recent initial conditions". Furthermore the fitting functions have to contain no more than two independent parameters (otherwise we have the over-fitting problem). The model satisfying to mentioned above conditions looks as follows:

1) A model intrinsic structure is given by the fixed relations between the fractions inside families of light and heavy nuclei:

$$f_p = w_p(p+\alpha) \ , \qquad f_{He} = w_{He}(p+\alpha) \ , \qquad w_p + w_{He} = 1 \ ,$$
$$f_N = w_N[1-(p+\alpha)] \ , \qquad f_{Si} = w_{Si}[1-(p+\alpha)] \ , \qquad f_{Fe} = w_{Fe}[1-(p+\alpha)] \ , \qquad w_N + w_{Si} + w_{Fe} = 1 \ . \tag{V.5}$$

In (V.5) $p+\alpha$ is the function of energy which should be found by experimental data processing. The function value at $E = 0.1$ PeV is known: $(p+\alpha)_{0.1 \text{ PeV}} = 0.56$.

2) The numbers w_A are:

$$w_p = \frac{25}{56} \ , \qquad w_{He} = \frac{31}{56} \ , \qquad w_N = \frac{19}{44} \ , \qquad w_{Si} = \frac{12}{44} \ , \qquad w_{Fe} = \frac{13}{44} \ . \tag{V.6}$$

3) The model is given by the choice of the dependence of the function $(p+\alpha)$ on energy. An experimental data fit (for a chosen model) has to lead to the value $\chi^2/dof \sim 0.1$ which is comparable to χ^2/dof obtained as a result of two-parameter fit of data with the supposition of a power type spectrum.

Below we discuss the two two-parameter models satisfying to enumerated conditions.

B. Linearly-logarithmic models with a linkage

In a simplest two-parameter model, the mass composition evolution in the region 1 PeV $\leqslant E \leqslant$ 10 PeV is given by a linearly-logarithmic function:

$$(p+\alpha)_E = (p+\alpha)_0' + (p+\alpha)_1' \ln \frac{E}{E_0'} \ , \qquad E_0' = 1 \text{ PeV} \ . \tag{V.7}$$

Numerical parameters $(p+\alpha)_0'$, $(p+\alpha)_1'$ are established on the base of experimental data processing:

$$(p+\alpha)_0' = 0.517 \pm 0.036 \ , \qquad (p+\alpha)_1' = 0.050 \pm 0.032 \ , \qquad \chi^2/dof = 0.115 \ . \tag{V.8}$$

The parameter Δ did not take part in fit. The value of $\Delta = 0.092$ has been chosen from the reasoning which will be presented below. The fitting curves constructed from the formulae (V.1) — (V.7) with parameters (V.8) do not visually distinguish from the curves plotted in Fig.1.

Next, in the region 0.1 PeV $\leqslant E \leqslant$ 1 PeV, the linearly-logarithmic model is given again but with others parameters one of which is known:

$$(p+\alpha)_E = 0.56 + (p+\alpha)_1 \ln \frac{E}{E_0} \ , \qquad E_0 = 0.1 \text{ PeV} \ . \tag{V.9}$$

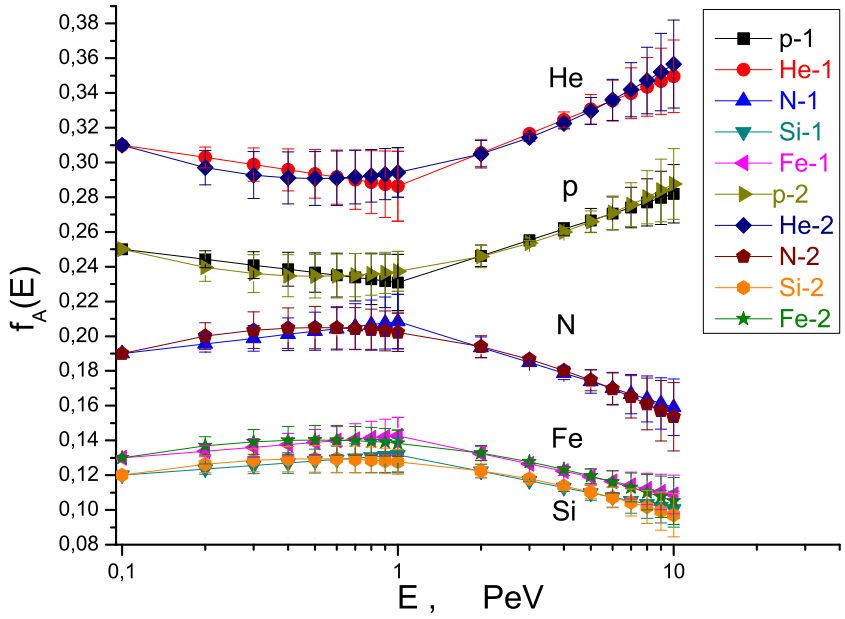

FIG. 3: The dependence of nuclei fractions on energy per a nucleus: 1 — Linearly-logarithmic models with a linkage (V.5) — (V.9); 2 — Quadratic logarithmic model (V.5), (V.6), (V.10), (V.11).

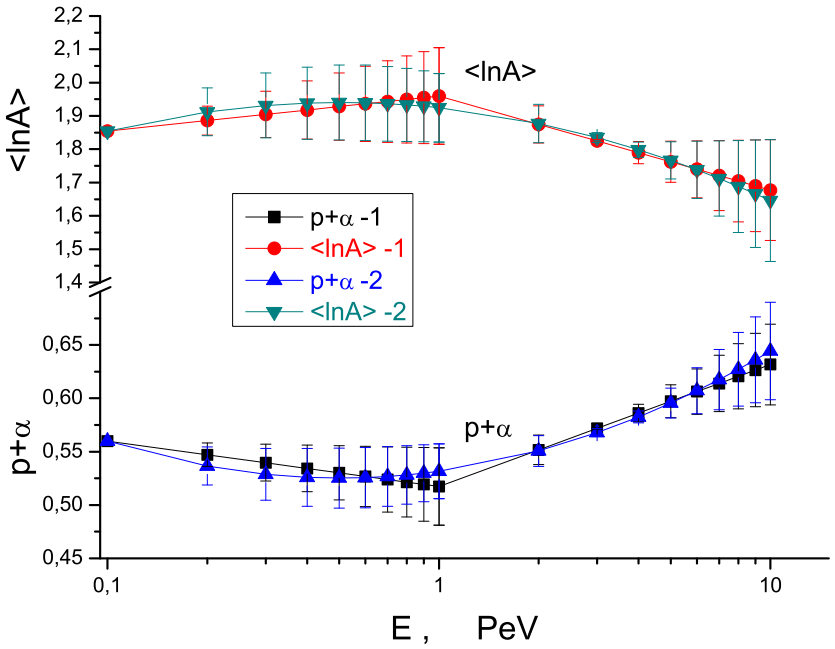

FIG. 4: The summary fractions of light nuclei and the mass number average logarithm vs energy per a nucleus: 1 — Linearly-logarithmic models with a linkage (V.5) — (V.9); 2 — Quadratic logarithmic model (V.5), (V.6), (V.10), (V.11).

The value of $(p+\alpha)_1$ is defined by means of a linkage of functions (V.7), (V.9) at $E = 1$ PeV:

$$(p+\alpha)_1 = \frac{1}{\ln 10}\left((p+\alpha)'_0 - 0.56\right) = -0.019 \pm 0.016 \ . \tag{V.10}$$

The nuclei fractions evolution in the energy range 0.1 PeV $\leqslant E \leqslant$ 10 PeV is presented in Fig.3. The quantities

$$(p+\alpha)_E \ , \qquad \langle \ln A \rangle_E = \sum_A f_A(E) \ln A \ .$$

are plotted in Fig.4. In these figures, the curves corresponding to linearly-logarithmic model are marked with index "1".

C. Quadratic logarithmic model

The nuclei fractions in the extended energy region 0.1 PeV $\leqslant E \leqslant$ 10 PeV can be approximated by quadratic functions in $\ln(E/E_0)$. In the model with intrinsic relationships (V.5), (V.6), the total fraction of light nuclei has the form:

$$(p+\alpha)_E = 0.56 + (p+\alpha)_1 \ln\frac{E}{E_0} + (p+\alpha)_2 \ln^2\frac{E}{E_0} \ , \qquad E_0 = 0.1 \text{ PeV} \ . \tag{V.11}$$

Coefficients $(p+\alpha)_1$, $(p+\alpha)_2$ are established by a fit of experimental data:

$$(p+\alpha)_1 = -0.043 \pm 0.032 \ , \qquad (p+\alpha)_2 = 0.013 \pm 0.009 \ , \qquad \chi^2/dof = 0.113 \ . \tag{V.12}$$

The value of $\Delta = 0.092$ corresponds to the best fit for this model. As in the linearly-logarithmic model, the fitting curves are undistinguishable from the curves presented in Fig.1. The nuclei fractions evolution and the mean logarithm of the mass number are shown in Fig.3, Fig.4. The corresponding curves are marked with index "2".

As is seen from figures 3, 4, two linearly-logarithmic models with a linkage and the quadratic logarithmic model in the extended energy region represent two (very close to each other) variants of the same model resulting in the same CR mass composition.

D. Mass composition reconstruction with the help of smoothed-out data

The use of smoothed-out data allows
1) first, to decrease the errors in nuclei fractions values,
2) secondly, to refuse from rigid relations between the fractions inside families of light and heavy nuclei.

The smoothed-out experimental data with interpolated errors in the multiplicity region $114 \leqslant n_\mu \leqslant 268$ are presented in Fig.5. It should be noted that after an error interpolation the error values are lowered by a factor equal to $\sqrt{P}$, where $P = 4$ is the number of primary experimental points subjected to a correction. A preliminary fit of smoothed-out data is carried out in the quadratic logarithmic model (V.11) with inside relations between the fractions (V.5), (V.6). The results are shown in Fig.5. We obtain the following values of fitted parameters:

$$(p+\alpha)_1 = -0.042 \pm 0.003 \ , \qquad (p+\alpha)_2 = 0.013 \pm 0.001 \ , \qquad \chi^2/dof = 0.008 \ . \tag{V.13}$$

We see that average values of fitted parameters (V.13), which have been obtained by the fit of smoothed-out data, coincide with the average values of the same parameters (V.12) obtained by means of the fit of input data. But uncertainties in the parameter values in (V.13) are an order less than in (V.12). This results in to a sharp fall of errors in the nuclei fraction values.

Note that the relative errors in final results of the two-parameter fit are about 10 %, this coincides with an order of magnitude of relative statistical errors of input experimental data (see the table II). This fact testifies that the reconstruction procedure is correct.[1]

---

[1] The point is the model parameters (except for the two sought values $(p+\alpha)_{1,2}$) are rigidly fixed, therefore if the procedure of experimental data treatment is mathematically correct then relative errors of required quantities and input data have to be comparable.

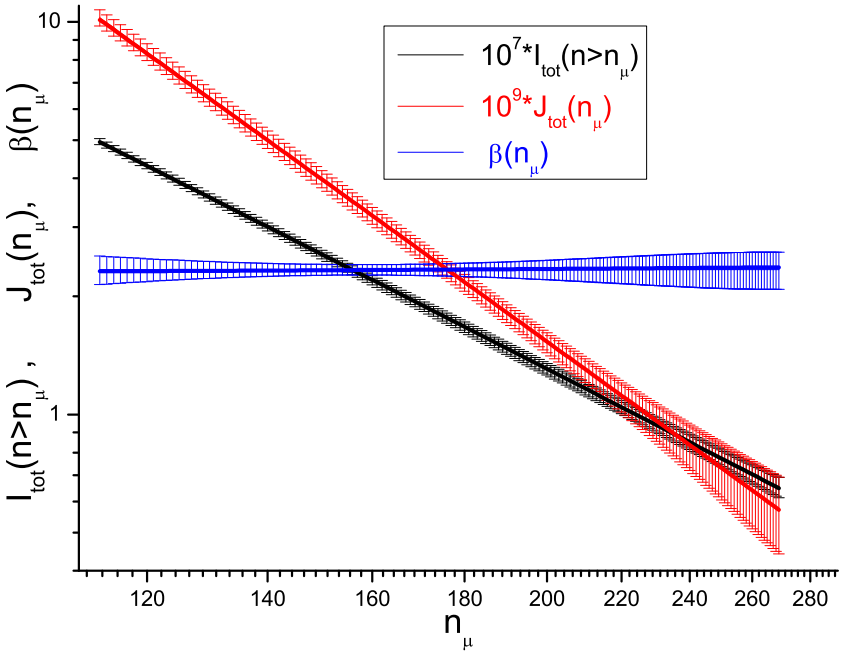

FIG. 5: Smoothed-out data constructed on the base of power spectrum (IV.7) with parameters (IV.8). The fit was carried out from the formulae (V.1) — (V.3) with the use of quadratic logarithmic model (V.16) with parameters (V.17).

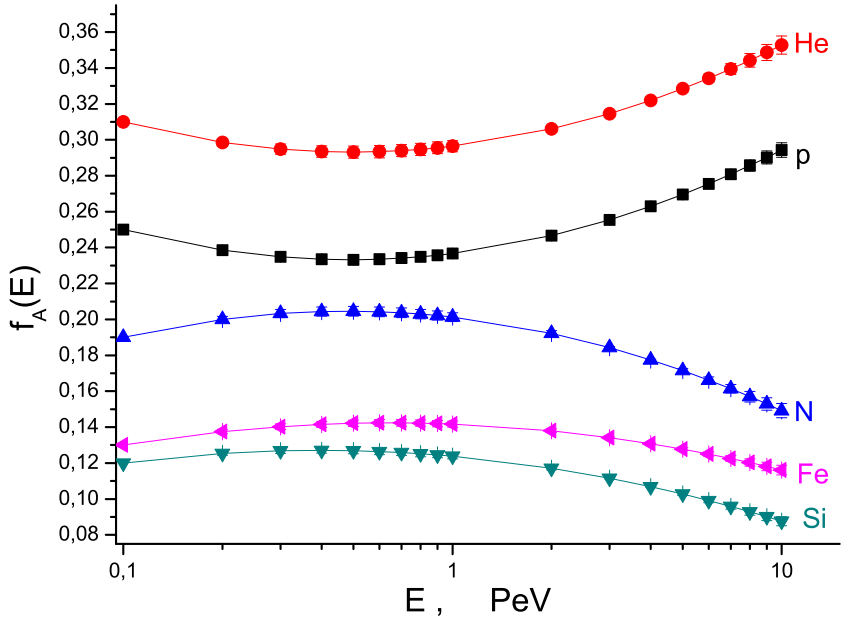

FIG. 6: The nuclei fractions dependence on the energy per a nucleus obtained by means of smoothed-out data processing shown in Fig.5. The mass composition reconstruction is performed with the quadratic logarithmic model (V.16) with parameters (V.17).

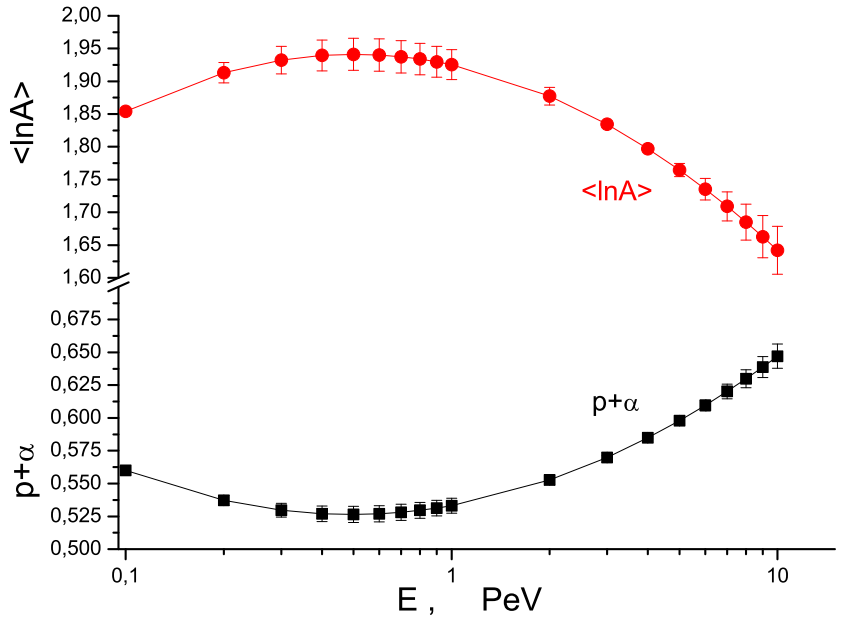

FIG. 7: The summary fraction of light nuclei $(p+\alpha)$ and the mass number average logarithm vs energy per a nucleus obtained by means of smoothed-out data processing shown in Fig.5. The reconstruction is performed with the quadratic logarithmic model (V.16) with parameters (V.17).

After a preliminary fit, the nuclei fraction values and its errors are calculated from the formulae

$$\begin{aligned} f_A &= w_A(p+\alpha)\ , \qquad {}_A = p,\quad {}_{He}\ , \\ f_A &= w_A[1-(p+\alpha)]\ , \qquad {}_A = {}_N,\quad {}_{Si},\quad {}_{Fe}\ , \end{aligned} \tag{V.14}$$

$$\Delta f_A = w_A \Delta(p+\alpha)\ , \qquad {}_A = p,\quad {}_{He},\quad {}_N,\quad {}_{Si},\quad {}_{Fe}\ , \tag{V.15}$$

where w_A are the numbers from (V.6); $(p+\alpha)_{1,2}$ are the numbers from (V.13). At the second stage of the fit, the nuclei fractions vary in the neighborhood of values (V.14) within the limits of uncertainties (V.15). Thus we use the quadratic logarithmic model detailed in fractions f_i:

$$\begin{gathered} f_A(E) = f_{A(0)} + f_{A(1)} \ln\frac{E}{E_0} + f_{A(2)} \ln^2\frac{E}{E_0}\ , \qquad E_0 = 0.1 \text{ PeV}\ , \\ \sum_A f_{A(1)} = 0\ , \qquad \sum_A f_{A(2)} = 0\ . \end{gathered} \tag{V.16}$$

We obtained the following values of fitted parameters:

$$\begin{aligned} f_{p(1)} &= -0.021 \pm 0.002\ , & f_{p(2)} &= 0.007 \pm 0.0004\ , \\ f_{He(1)} &= -0.021 \pm 0.002\ , & f_{He(2)} &= 0.007 \pm 0.0005\ , \\ f_{N(1)} &= 0.019 \pm 0.002\ , & f_{N(2)} &= -0.006 \pm 0.0004\ , \\ f_{Si(1)} &= 0.010 \pm 0.001\ , & f_{Si(2)} &= -0.004 \pm 0.0003\ , \\ f_{Fe(1)} &= 0.013 \pm 0.001\ , & f_{Fe(2)} &= -0.004 \pm 0.0003\ , \\ \chi^2/dof &= 0.008\ . \end{aligned} \tag{V.17}$$

Nuclei fractions evolution with energy is shown in Fig.6. The combined fraction of light nuclei and the mass number average logarithm are presented in Fig. 7. Comparison of results presented in Figs.6, 7 and in Figs.3, 4 shows that the

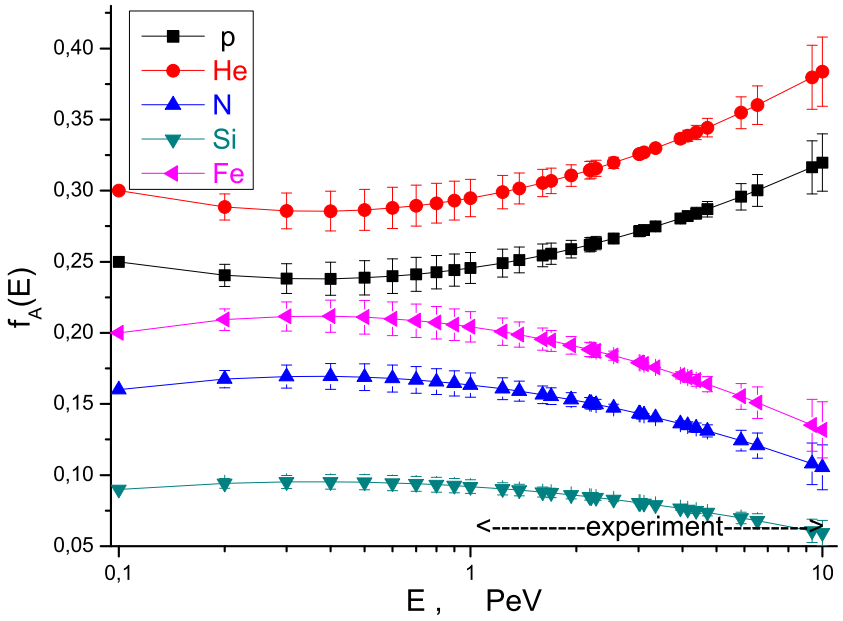

FIG. 8: The nuclei fractions dependence on the energy per a nucleus obtained by means of experimental data processing shown in Fig.1. The mass composition reconstruction is performed with the quadratic logarithmic model (V.11), (V.5) with parameters (V.19).

mass composition reconstructed from smoothed-out data is in the error band of the mass composition reconstructed from the input data.

E. Others "initial conditions"

Initial conditions (i.e. the nuclei fractions at $E_0 = 100$ TeV) have to be given by direct measurements on satellites or stratosphere balloons. The most recent resume of such measurements is presented in [8]. These data selection on nuclei groups gives

	p	He	CNO	Ne-S	Fe
A	1	4	14	28	56
$f, \%$	25	30	16	9	20

(V.18)

Within the framework of quadratic logarithmic model (V.11), (V.5) with parameters

$$w_p = \frac{25}{55}\,, \qquad w_{He} = \frac{30}{55}\,, \qquad w_N = \frac{16}{45}\,, \qquad w_{Si} = \frac{9}{45}\,, \qquad w_{Fe} = \frac{20}{45}\,, \tag{V.19}$$

we have obtained the following values of fitted parameters:

$$(p+\alpha)_1 = -0.042 \pm 0.030\,, \qquad (p+\alpha)_2 = 0.016 \pm 0.009\,, \qquad \chi^2/dof = 0.130\,. \tag{V.20}$$

As is seen from the comparison (V.20) with (V.13), the values of fitted parameters (corresponding to models with different initial conditions) are consistent with each other within the limits of statistical uncertainties of the fit. The energy evolution of nuclei fractions is shown in Fig.8. In Fig.9 the fraction of light nuclei and the mass number average logarithm are presented for two variants of initial conditions (V.4) and (V.18). As is seen, the mass composition characteristics $(p+\alpha)$ and $\langle\, lnA\rangle$ are practically the same for initial condition variants discussed above. Let us remark here that the mass composition evolution obtained in this work is in good agreement with averaged results reported in [6].

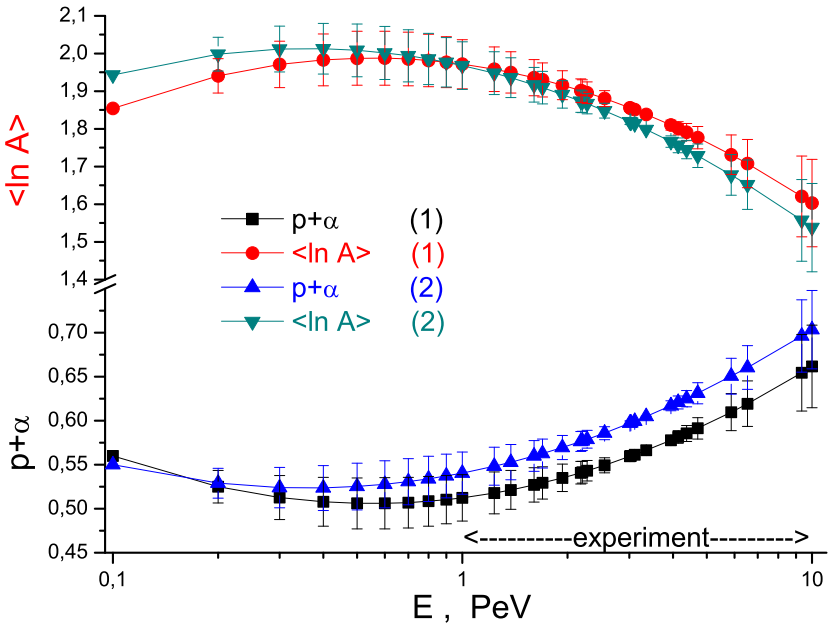

FIG. 9: The summary fraction of light nuclei $(p + \alpha)$ and the mass number average logarithm vs energy per a nucleus obtained by means of experimental data processing shown in Fig.1. The reconstruction is performed with the quadratic logarithmic model (V.11), (V.5): **(1)** — initial conditions (V.4) with parameters (V.17), **(2)** — initial conditions (V.18) with parameters (V.19).

VI. THE DEPENDENCE OF AVERAGE NUMBER OF MUONS ON THE EAS ENERGY

We return to the formula (III.7) of Section III B. Now we know the mass composition and can verify the identity (III.7) assuming that the energy $E_A(n_\mu)$ (see (III.5)) coincides with the average energy $\overline{E}_A(n_\mu)$. A verification reduces to the calculation of right part of the expression (III.7) for the mass composition given by the model (V.16) with parameters (V.17):

$$n_\mu^{(calc)} = \sum_A f_A[E_A(n_\mu^{(det)})] \cdot n_\mu^{(A)}[E_A(n_\mu^{(det)})] \ , \tag{VI.1}$$

$$n_\mu^{(A)}[E_A(n_\mu)] = n_A(E_0) \cdot \left(\frac{E_A(n_\mu^{(det)})}{E_0} \right)^{\zeta_A} \tag{VI.2}$$

here $n_\mu^{(det)}$ is the value of muon number obtained in our experiment. We use in calculations the numbers listed in the table IV. The results are presented in Fig.10. The numbers $n_\mu^{(det)}$ have errors related to the Monte-Carlo simulation of the parameter $\Delta(m)$. Calculated values $n_\mu^{(calc)}$ have errors corresponding to small uncertainties in values of fractions $f_A(E)$. As is seen from Fig.10, the numbers $n_\mu^{(calc)}$ obtained from the formula (VI.1) are slightly different from $n_\mu^{(det)}$. Generally speaking, there are two reasons for these differences: 1) errors in the mass composition determination, 2) inaccuracies in formulae (VI.2) related to an identification $E_A(n_\mu)$ and $\overline{E}_A(n_\mu)$ energies. We believe the second reason is more likely. Let us suppose that these energies are related by means of the simplest relationship

$$\overline{E}_A(n_\mu) = k \cdot E_A(n_\mu) \ , \tag{VI.3}$$

where k is a universal (for an energy region under consideration) factor common for all nuclei. In this case in (VI.2) one must make the substitution $E_A(n_\mu) \to k \cdot E_A(n_\mu)$ following which the formula for the average number of muons

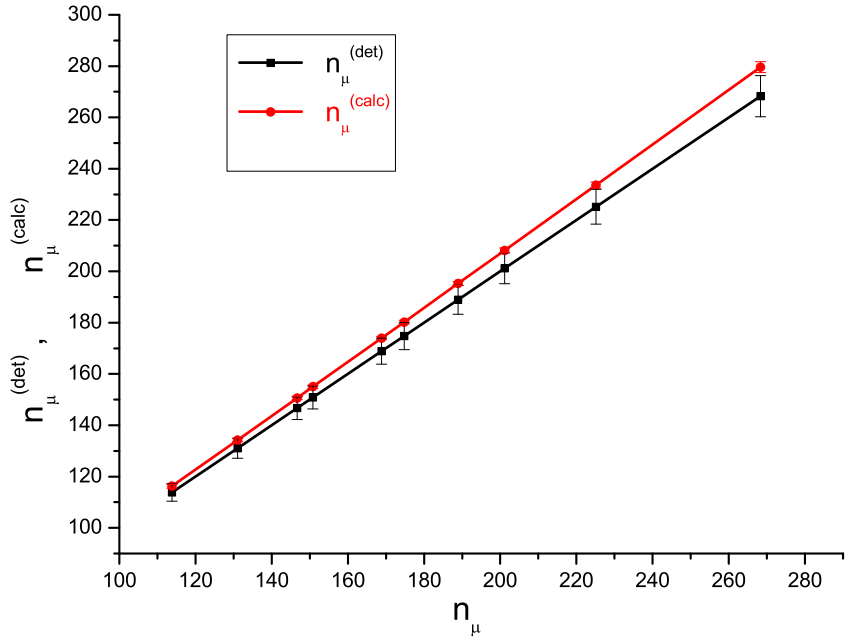

FIG. 10: $n_\mu^{(det)}$ and $n_\mu^{(calc)}$ numbers of high energy muons according to (VI.1), (VI.2) with energies $E_A(n_\mu^{(det)})$ from he table IV. The mass composition model (V.16) with parameters (V.17) is used.

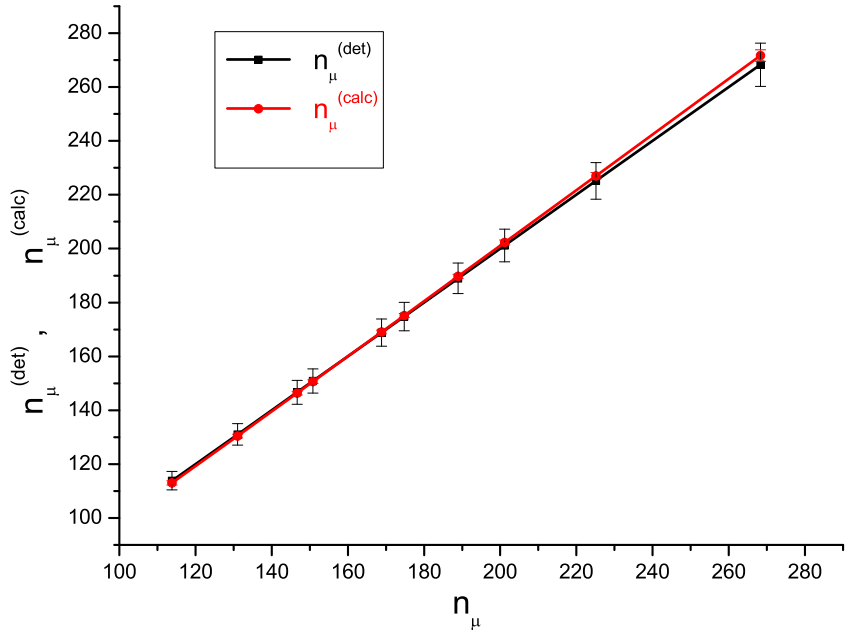

FIG. 11: corrected $n_\mu^{(calc)}$ and $n_\mu^{(det)}$ numbers of high energy muons according to (VI.1), (VI.4). The mass composition model (V.16) with parameters (V.17) is used.

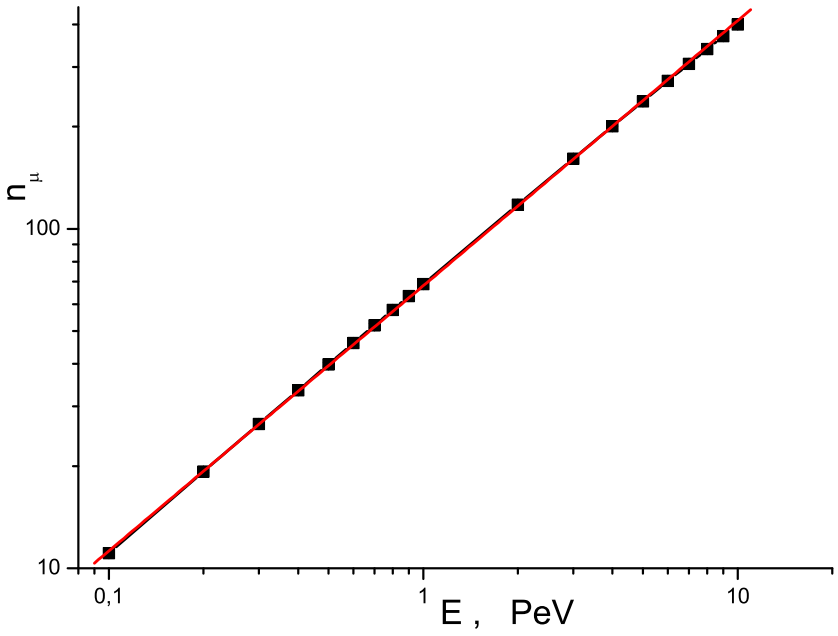

FIG. 12: The average number of high energy muons ($E_\mu \geqslant 235$ GeV) in EAS as a functional of the CR mass composition. Conditional "experimental" points are calculated from the formulae (VI.1), (VI.4). The mass composition model (V.16) with parameters (V.17) is used. The fitting curve is constructed according to (VI.6).

takes the form

$$n_\mu^{(A)}[E_A(n_\mu^{(det)})] = k^{\zeta_A} n_A(E_0) \cdot \left(\frac{E_A(n_\mu^{(det)})}{E_0} \right)^{\zeta_A} . \tag{VI.4}$$

The results of calculations from the formulae (VI.1), (VI.4) at $k = 0.964$ are presented in Fig.11. Thus we can get a practical coincidence of $n_\mu^{(calc)}$ and $n_\mu^{(det)}$ numbers by means of matching the factor $k \sim 1$.

The average number of muons ($E_\mu \geqslant 235$ GeV) produced by EAS with energy E and the mass composition $f_A(E)$ is given by the expression:

$$\begin{gathered} n_\mu(E) = \sum_A f_A(E) \cdot n_\mu^{(A)}(E) = \sum_A k^{\zeta_A} n_A(E_0) \cdot f_A(E) \cdot \left(\frac{E}{E_0} \right)^{\zeta_A} , \\ \sum_A f_A(E) = 1 . \end{gathered} \tag{VI.5}$$

The plot of the function $n_\mu(E, E_\mu \geqslant 235$ GeV) for the mass composition model (V.16) with parameters (V.17) is shown in Fig.12. As it has turned out, the curve ready-built from the formula (VI.5) is ideally described by the power function

$$\begin{gathered} n_\mu(E) = n_{tot}(E_0) \left(\frac{E}{E_0} \right)^{\zeta} , \\ E_0 = 0.1 \text{ PeV} , \qquad n_{tot}(E_0) = 11.246 \pm 0.049 , \qquad \zeta = 0.781 \pm 0.001 . \end{gathered} \tag{VI.6}$$

that lends support to the validity of data processing (see also Appendix B).

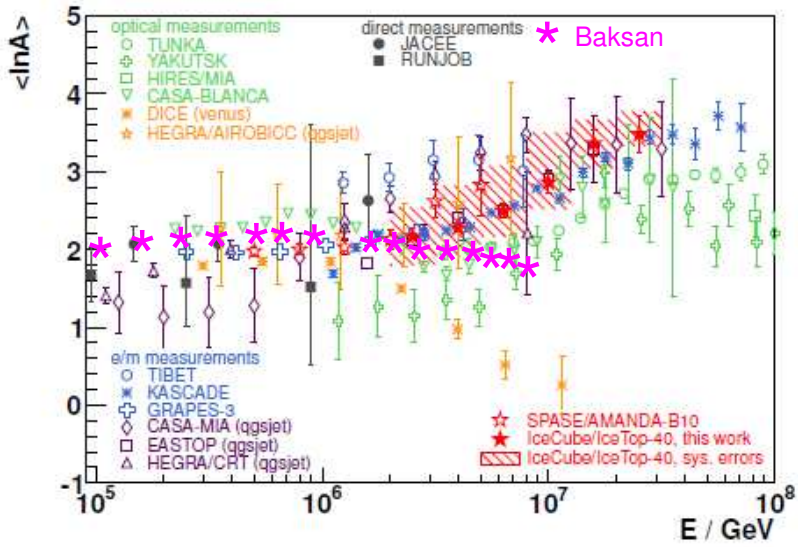

FIG. 13: The mass number average logarithm vs energy per a nucleus reported in a number papers. Baksan results are plotted on the graph from the paper [9].

VII. DISCUSSION AND CONCLUSION

We have presented the new method of the analysis of data on the Extensive Air Showers spectrum versus the total number of high energy muons that allows us to trace the dependence of the mass composition on the energy. We have introduced the notion of secondary experimental data and proved the smoothing procedure. This has made it possible to obtain the information on the energy dependence of CR mass composition in the region of $0.1 - 10$ PeV.

As is seen from above, the results obtained within the framework of linearly-logarithmic model and quadratic logarithmic model are the same practically. An evolution of PCR mass composition in the energy region $0.1 - 10$ PeV is shown in Fig.6, Fig.7. One can see a good agreement the present results with the ones obtained in [6] in which the mass composition averaged over the region under discussion was determined.

In Fig.13 the data on the mean logarithmic mass vs primary energy obtained in this paper are compared with the ones reported in a number of others experiments. Our data point to nonmonotonic energy dependence of CR mass composition. We see some lightening of the mass composition in the region > 1 PeV (it may be related with an acceleration mechanism of cosmic rays in supernova shells).

A distinguishing feature of our method of the mass composition determination is its weak dependence on assumptions concerning nuclei interaction models at high energies. Of all characteristics of interactions, we use only one characteristic – statistical distribution of high energy muons (arising in primary interactions) on the energy and multiplicity. It is known from accelerator data that this is the negative binomial distribution (NBD) having two intrinsic parameters – the average (in distribution) muon number $n_\mu^{(A)}(E)$, producing in primary interactions, and a parameter $k_A(E)$ characterizing a distribution variance. The two parameters are the functions of energy and mass number of a nucleus. To calculate this functions it takes indeed a model interaction attraction. We use NBD with functions $n_\mu^{(A)}(E)$, $k_A(E)$ approved in previous works.

Appendix A

The negative binomial distribution is a discrete probability distribution of the number of successes in a sequence of Bernoulli trials before a specified (non-random) number k of failures occurs

$$B(k,p) = C_r^{r+k-1}(1-p)^k p^r, \quad k = 0,1,2,... \tag{A.1}$$

here p is the probability of success.

Putting $r = n_\mu$ and taking into account $\overline{n}_\mu = kp/(1-p)$ we obtain

$$B(n_\mu, \overline{n}_\mu, k) = C_{n_\mu}^{n_\mu+k-1} \left(\frac{\overline{n}_\mu/k}{\overline{n}_\mu/k+1}\right)^{n_\mu} \frac{1}{(\overline{n}_\mu/k+1)^k} \tag{A.2}$$

The parameter k was chosen in the form obtained in [14]

$$k = \frac{\overline{n}_\mu}{f^2-1}, \quad f = A^{0.06}\left(1+0.013\frac{E_o}{E}\right)^{0.18} \tag{A.3}$$

At such choice of k the variance of $B(n_\mu, \overline{n}_\mu, k)$ distribution is greater than the one of Poisson distribution in $6-10$ times for protons and $2-3$ times for iron nuclei in the energy region under discussion in accordance with results of others works (e.g. [10, 11]).

Appendix B

To calculate the parameters $\Delta(m)$ and $G(m)$ [4, 12], we have used Monte-Carlo simulation and the approximation of spatial-energy distribution function (SDF) of muons in EAS obtained in [13],

$$f(r, \geqslant E, E_o) = C \times exp[-(r/r_o)^d], \tag{B.1}$$

here

$$r_o = \frac{0.95}{(1+12.5E)^{0.92}} + \frac{0.42}{E^{1.23}E_o^{0.9}}, \quad d = 0.43 + \frac{0.2}{0.2+E_o},$$

E_o is an energy per nucleon in a primary nucleus, E is the muon threshold energy (E in TeV, r in meters), C - a normalization factor.

The muon density ρ at a distance r from EAS axis is defined by the expression

$$\rho(r, \geqslant E, E_o)2\pi r dr = \overline{n}_\mu(A, E_o, \geqslant E) f(r, E_o, \geqslant E) r dr, \tag{B.2}$$

here $\overline{n}_\mu$ is the average number of muons with energy $\geqslant E$ produced by a primary nucleus with energy $E_N = AE_o$ (A is the number of nucleons in a nucleus) [13]:

$$\overline{n}_\mu(A, E_o, \geqslant E, \theta) = \frac{0.0187 Y(\theta) A}{E^a}\left(\frac{E_o}{E}\right)^{0.781}\left(\frac{E_o}{E_o+E}\right)^{\delta}, \tag{B.3}$$

where E_o and E in TeV,

$$a = 0.9 + 0.1lg(E), \quad \delta = E + \frac{11.3}{lg(10+0.5E_o)}, \quad Y(\theta) = \frac{1+0.36\times ln(\cos\theta)}{\cos\theta},$$

θ — zenith angle.

[1] Alexeev E.N. et al., Proc. 16th ICRC, Kyoto, 1979, v. 10, p.276.
[2] Voevodsky A.V. et al., Rus.J. Izvestiya of RAS, ser.phys., v.58, N 12, p.127, 1994
[3] Bakatanov V.N., Novoseltsev Yu.F., Novoseltseva R.V. Astropart. Phys. 12 (1999) 19
[4] Yu.F. Novoseltsev. Rus.J. Nuclear Physics, v.63, N 6, p.1129, 2000
[5] V.N. Bakatanov, Yu.F. Novoseltsev, R.V. Novoseltseva. Proc. 27th ICRC, Hamburg 2001, v.1, p.84
[6] Novoseltsev Yu F, Novoseltseva R V and Vereshkov G M (2012) J. Phys. G: Nucl. Part. Phys. 39, 105202
[7] Amenomori M. et al 1995 Proc. 24th Int. Cosmic Ray Conf. (Rome) v.2 p.736
[8] K. Nakamura et al., J.Phys. G 37, 075021 (2010).
[9] K.-H. Kampert and M. Unger, Astroparticle Physics 35, 660 (2012).
[10] Bilokon H. et al. Proc. XXI ICRC, 1990, Adelaide, v.9, p.366
[11] Attallah R. et al. Proc. XXIV ICRC, 1995, Rome, v.1, p.573
[12] Novoseltsev Yu.F. Doctor of Sciences Thesis, Institute for Nuclear Research of RAS, Moscow, 2003
[13] Boziev S.N., Voevodsky A.V., Chudakov A.E.. Preprint P-0630, Institute for Nuclear Research of RAS, 1989
[14] Boziev S.N. Sov. J. Nuclear Physics, 52 (1990) 500.